

A Stability Analysis of Tropical Ocean–Atmosphere Interactions: Bridging Measurements and Theory for El Niño

ALEXEY V. FEDOROV AND S. GEORGE PHILANDER

Atmospheric and Oceanic Sciences Program, Department of Geosciences, Princeton University, Princeton, New Jersey

(Manuscript received 12 September 2000, in final form 2 January 2001)

ABSTRACT

Interactions between the tropical oceans and atmosphere permit a spectrum of natural modes of oscillation whose properties—period, intensity, spatial structure, and direction of propagation—depend on the background climatic state (i.e., the mean state). This mean state can be described by parameters that include the following: the time-averaged intensity τ of the Pacific trade winds, the mean depth (H) of the thermocline, and the temperature difference across the thermocline (ΔT). A stability analysis by means of a simple coupled ocean–atmosphere model indicates two distinct families of unstable modes. One has long periods of several years, involves sea surface temperature variations determined by vertical movements of the thermocline that are part of the adjustment of the ocean basin to the fluctuating winds, requires a relatively deep thermocline, and corresponds to the delayed oscillator. The other family requires a shallow thermocline, has short periods of a year or two, has sea surface temperature variations determined by advection and by entrainment across the thermocline, and is associated with westward phase propagation. For the modes to be unstable, both families require that the background zonal wind exceed a certain intensity. An increase in ΔT , and in H beyond a certain value, are stabilizing. For intermediate values of H , between large values that favor the one mode and small values that favor the other, the modes are of a hybrid type with some properties of each family. The observed Southern Oscillation has been of this type for the past few decades, but some paleorecords suggest that, in the distant past, the oscillation was strictly of the delayed oscillator type and had a very long period on the order of a decade.

1. Introduction

Numerous studies over the past two decades of the interactions between the tropical oceans and the atmosphere have advanced our understanding of El Niño and associated phenomena enormously. (See June 1998 of *J. Geophys. Res.*, **103** (C7) for a series of excellent review articles.) A number of issues nonetheless remain problematic, especially the relevance of theoretical results concerning the stability of the ocean–atmosphere interactions to the interpretation of measurements. For example, in their recent summary of measurements, the view that McPhaden et al. (1998) take of El Niño is somewhat different from that of Neelin et al. (1998) in the companion paper that reviews theoretical results. Whereas the latter authors explain the Southern Oscillation as a natural mode of oscillation of the coupled system—as an eigenvalue problem—McPhaden et al. (1998), although describing the basic theoretical ideas from the other paper and recognizing the complexity of

the coupled system, put more emphasis on the possible initiation of developments by random westerly wind bursts. There have been occasions when wind bursts appear to influence the development of El Niño, but at other times they failed to do so and, some times, El Niño develops in their absence. Why is the impact of westerly wind bursts so different at different times? What observations should one look at to better test the available theories? The answers require a better understanding of the stability properties of the modes. Presumably wind bursts are of primary importance when ocean–atmosphere interactions give rise to neutrally stable or damped modes, but play a minor role should the interactions be sufficiently unstable for the natural modes to be self-sustaining. What are the necessary conditions for instability? What parameters determine whether the natural modes are damped or self-sustaining? Surprisingly, these questions, at present, have no easily accessible answers in terms of readily measurable quantities such as the zonally averaged depth of the thermocline, or the mean intensity of the winds. Nor is there information about changes in the structure of the modes in response to changes in the values of those parameters. Neelin et al. (1998) describe a variety of possible modes that range from the delayed oscillator

Corresponding author address: Dr. Alexey Fedorov, Philander, Atmosphere and Oceanic Sciences Program, Department of Geosciences, Princeton University, Sayre Hall, P.O. Box CN710, Princeton, NJ 08544.
E-mail: alexey@princeton.edu

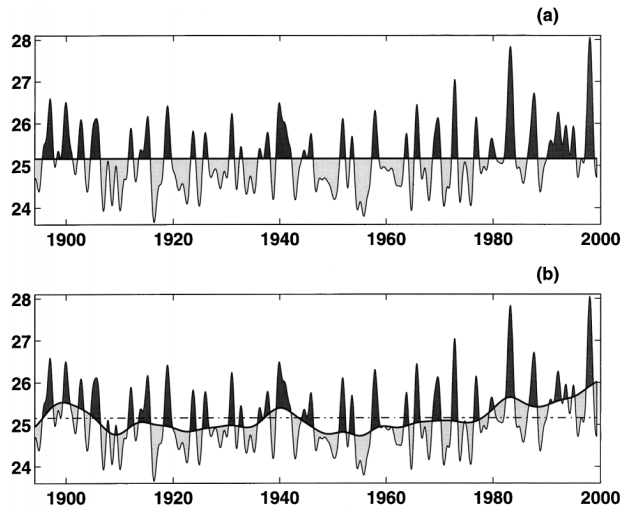


FIG. 1. The interannual oscillations in SST (in $^{\circ}\text{C}$) at the equator in the eastern Pacific (averaged over the area 5°S – 5°N , 80° – 120°W) are shown on the background of (a) the time-averaged temperature for the century (b) the low-frequency interdecadal changes. The plots are obtained by applying, to the available measurements, two different low-pass filters with the cutoff frequencies of approximately 0.9 and 0.09 yr^{-1} . The darker (lighter) part of the graph indicates El Niño (La Niña).

with a timescale dependent on the processes of oceanic adjustment, to “SST” modes with timescales that depend on processes such as advection and upwelling that directly influence sea surface temperatures. They conclude that the observed Southern Oscillation is a hybrid of these types. Is it possible that the composition of the hybrid is different at different times, mostly delayed oscillator some of the time, SST mode at other times?

The answers to these questions are of direct relevance to the current debate concerning the sea surface temperature fluctuations shown in Fig. 1a—seasonal and higher-frequency variations have been filtered from these measurements in the eastern tropical Pacific. This record shows that, during the decades leading up to the 1960s, El Niño occurred sporadically, but then became more regular with a period of approximately 3 yr. (Changes in the dominant period and regularity of the Southern Oscillation are also evident in the wavelet spectral analysis of the unfiltered temperature record in Fig. 2.) Since the 1980s the period seems to have increased to 5 yr approximately, but the cold La Niña episodes have practically disappeared. The two most intense episodes in the entire records, those of 1982 and 1997, occurred during the past two decades. Could global warming be the cause of these recent changes in the properties of the Southern Oscillation? Some investigators (Trenberth and Hoar 1997) answer in the affirmative but others contend that the time series is stationary and reflects the impact of random disturbances, mainly of atmospheric origin, on a regular oscillation attributable to ocean–atmosphere interactions (Harrison

and Larkin 1997; Wunsch 1999; Rajagopalan et al. 1997).

Thus far, this debate about Fig. 1a has focused on statistical issues. A complementary approach, that pays attention to the physical processes involved, is to explore how changes in the background state, attributable to global warming or some other long-term climate change, affect the Southern Oscillation. Such an approach implies that the choice of the time-averaged temperature of the past century as a reference line in Fig. 1a is arbitrary because the reference temperature is an aspect of the background climate state which, in reality, is changing continually. The choice of the interdecadal fluctuation, obtained by low-pass filtering the data, as reference line gives a new perspective on the interannual variability as is evident in Fig. 1b. Now the apparently prolonged El Niño that started in 1992 amounts merely to a persistence of background conditions, the episodes of 1982 and 1997 appear less exceptional than in Fig. 1a, and La Niña is present throughout the record, even during the past two decades. A key aspect of the decadal fluctuation of the background state—it has been documented by Guilderson and Schrag (1998), Zhang et al. (1997), Chao et al. (2000), and Giese and Carton (1999)—is the gradual warming of the eastern tropical Pacific since the 1960s. The cause of that warming is a matter of debate. To some it is merely a by-product of the El Niño irregularity (Kirtman and Schopf 1998; Thompson and Battisti 2000), so that there is no reason to expect any difference between the physical processes that determine the interannual and decadal variability. Others (Gu and Philander 1997; McCreary and Lu 1994) propose that exchanges between the Tropics and extratropics can result in self-sustaining decadal fluctuations. This paper is concerned, not with the origin of the decadal fluctuation, but with its effect on the interannual variations. That effect is determined by means of a stability analysis of different background states (i.e., different mean states). The results shed light not only on the past 100 yr, but also on the differences between El Niño as simulated by different climate models, and on climate records from the distant past, for example on the record of sediments from a lake in southwestern Ecuador (Rodbell et al. 1999), which suggests that the Southern Oscillation was established (or reestablished) only 5000–7000 yr before present.

Although the tools to be used in this study are standard—a coupled ocean–atmosphere model of the type developed by Zebiak and Cane (1987); stability analyses similar to those employed by Jin and Neelin (1993)—and although the modes to be discussed are those previously investigated by others—see Neelin et al. (1998) for a review—the perspective taken here is novel, and new results emerge. Previous results concerning the different types of ocean–atmosphere modes do of course remain valid, but we will argue that a redefinition of terms such as “delayed” oscillator is desirable. One goal of this paper, bridging the gap that at present sep-

Wavelet Spectral Density

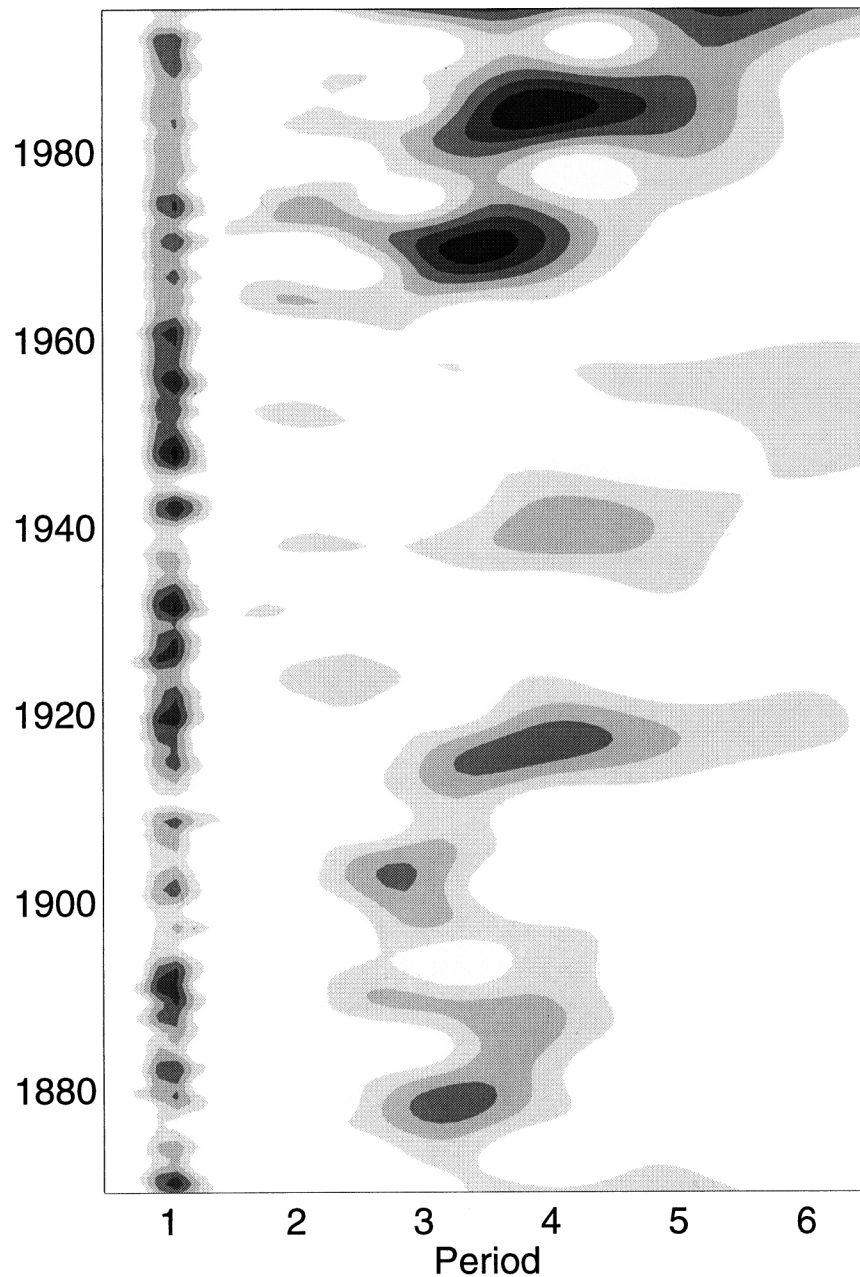


FIG. 2. Energy density, from a wavelet spectral analysis, as a function of period and time for the SST signal used in Fig. 1. Dark (light) shading corresponds to high (low) values, respectively. The spectral density for the annual cycle is large from 1920 to 1960, whereafter the interannual oscillations increase in amplitude.

arates observational and theoretical studies, motivates us to examine the stability characteristics of different mean states by varying, not the values of nondimensional parameters, but rather the time-averaged intensity τ of the Pacific trade winds, the mean depth H of the thermocline (i.e., zonally and time averaged), and the temperature difference ΔT across the thermocline. By

doing so, we can establish necessary conditions for instability of ocean-atmosphere interactions in a form equivalent to those available for, say, baroclinic instability where the vertical shear of the flow and the latitudinal thermal gradient are the critical parameters.

One of the main results to emerge from this study, and a companion paper by Fedorov (2001) is that the

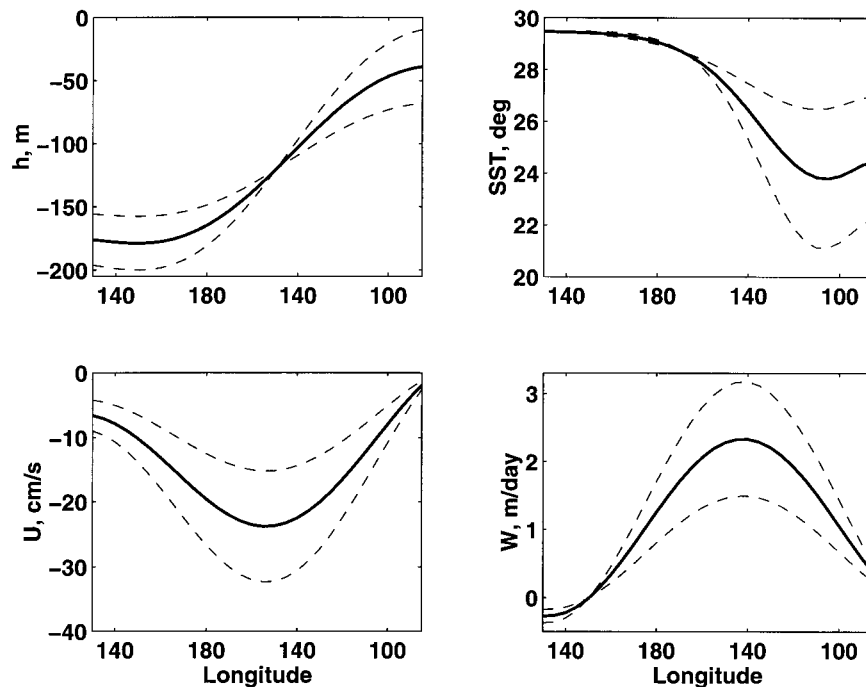


FIG. 3. A typical mean state calculated by the model (solid lines), and the margins within which changes occur for varying τ (dashed lines), for $H = 120$ m, $\Delta T = 7^\circ\text{C}$. To produce the dashed lines, the intensity of the wind was increased/reduced by about 40%. Stronger winds (i.e., larger τ) result in greater thermocline slope and temperature gradient, and stronger zonal current and upwelling.

different perspectives of McPhaden et al. (1998) and Neelin et al. (1998) as regards El Niño, are complementary. The results in this paper indicate that the Southern Oscillation is a marginally unstable (or possibly weakly damped) natural mode—its period is on the order of 5 yr at present so that it has to be sustained by random perturbations such as the westerly wind bursts that sporadically appear on the equator near the date line. Records such as that in Fig. 1 therefore involve several timescales that include the period of the interannual natural mode of oscillation, and the time of the oceanic response to wind bursts. Although the oceanic Kelvin waves associated with the latter response are frequently cited as being of critical importance to the development of El Niño, that is not the case. Such waves are indeed present, and propagate rapidly across the Pacific, but of far greater importance is the coupled ocean–atmosphere response to wind bursts. That response, which can move eastward across the Pacific on a timescale longer than that of oceanic Kelvin waves, but shorter than the natural modes of oscillation, often corresponds to “nonnormal modes” of the type discussed by Moore and Kleeman (1997, 1999).

2. The model

This study uses a coupled ocean–atmosphere model similar to those of Zebiak and Cane (1987), Battisti and

Hirst (1989), and Jin and Neelin (1993). The oceanic component is a shallow-water model with an embedded mixed layer and spatially varying sea surface temperature (SST) determined by a parameterized advection–diffusion equation. For simplicity, we assume that the important dynamics are confined to the immediate vicinity of the equator, which is taken to be a line of symmetry, and we ignore the seasonal cycle. A modified shallow-water atmosphere responds to the SST variations and provides the winds that drive the ocean. A full description of the model, along with the main differences from Jin and Neelin (1993), hereafter referred to as JN, are given in appendix A.

The model concerns departures from a specified background climate state that depends upon many different processes in the Tropics and beyond. Of the parameters that describe that state, H , τ , and ΔT (defined above) are of special interest. Once their values are specified, then it is necessary to calculate the dynamically consistent oceanic currents, the slope of the thermocline, and sea surface temperature. A change in the values of τ , H , and ΔT —a transition from one physically realizable state to another—is likely to involve changes in several parameters. For example, an increase in thermocline depth, should it be accompanied by a smaller SST gradient along the equator, leads to weaker winds, and therefore a smaller slope for the thermocline. This study oversimplifies these ocean–atmosphere interac-

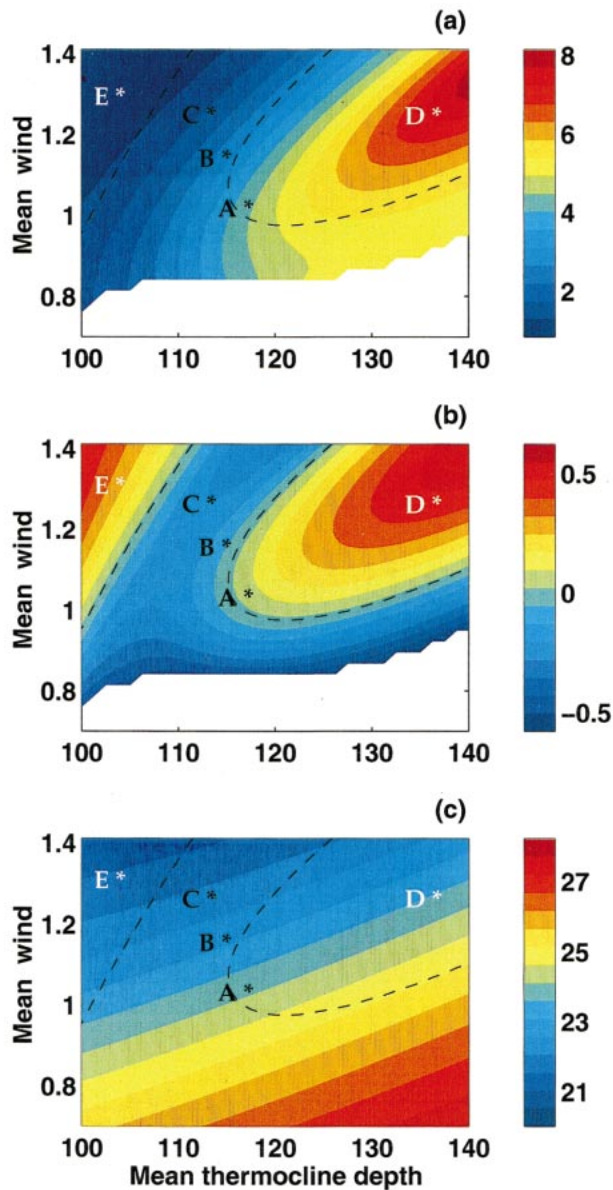


FIG. 4. Changes in (a) the period and (b) growth rates of the most unstable oscillations as a function of changes in the easterly winds along the equator (in the units of 0.5 dyn cm^{-2}), and in the depth of the equatorial thermocline (m). The value of ΔT measured over a 50-m depth variation is 7°C . The dotted line corresponds to the line of zero growth rate; in the white area both amplifying and damped modes are absent. (c) The minimum SST (in $^\circ\text{C}$) of the basic state in the eastern Pacific Ocean.

tions and assumes that the SST produced by the wind can in turn generate that wind. In reality there are feedbacks, similar to those involved in El Niño, that determine the mean state. [See Dijkstra and Neelin (1995, 1999) for a discussion.] Those feedbacks are disregarded in this model.

Examples of the mean states provided by the model are shown in Fig. 3. The model captures the observed variations in the depth of the thermocline and the SST

distribution along the equator reasonably well, and gives reasonable changes in the characteristics of the mean state due to changes in H (or ΔT). The surface velocity is somewhat different from the observed values but only in the western Pacific Ocean, which does not significantly affect the properties of the interannual variability.

After determination of a dynamically consistent background state, the next step is a linear stability analysis similar to that of Battisti and Hirst (1989), and Jin and Neelin (1993). The analysis is performed for many different background states to produce the eigenvalues and eigenfunctions, yielding the structure and the properties of the modes. To check the validity of the linear approach the model was also run in a time-dependent mode, in a fully nonlinear regime; the comparison showed that the nonlinear solutions are very similar to the linear modes at low to moderate growth rates.

The model has a large number of parameters, in addition to those already mentioned (see appendix A). The values assigned to the various parameters are such that, for values of τ , H , and ΔT appropriate for the period 1980 onward, the simulated Southern Oscillation is as close as possible (in period, etc.) to the oscillation observed since the 1980s. In other words, the model has been tuned to be realistic for the period from 1980 onward. Those values for the different parameters were then kept constant in sections 3–5 where only the values of τ , H , and ΔT are varied to study the effect of changes in background conditions.

The actual procedure of the analyses is as follows. After τ , H , and ΔT are specified, the model is run in a nonlinear regime to calculate oceanic currents, the slope of the thermocline, sea surface temperature, and upwelling. Then the equations of motion and temperature balance are linearized (numerically) with respect to a predetermined mean state. The last part of the procedure is calculating (again numerically) the eigenvalue and eigenfunction for the most unstable (or the least damped) mode. The eigenvalues give the period and growth rates of the oscillations (if any exist), while the corresponding eigenfunction gives the spatial structure of the mode. Next, the calculations are repeated for different τ , H , or ΔT .

In this analysis we study the normal modes of the system. At a specific time, the response of the ocean–atmosphere to a burst of westerly winds say, will involve, not necessarily those modes, but instead the so-called “nonnormal modes” (e.g., Moore and Kleeman 1997, 1999) whose structures are in part determined by conditions at the time of the wind bursts. Those conditions depend on the phase of the background, interannual oscillation corresponding to the normal mode. [The responses to westerly wind bursts are different at the peaks of El Niño and La Niña. See Fedorov (2001).]

3. Stability properties

The most unstable natural modes of oscillation have periods and growth rates whose dependence on the val-

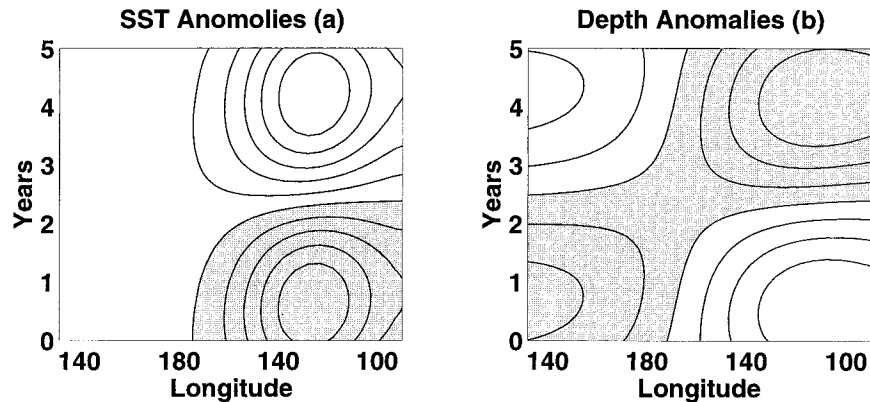


FIG. 5. The time-space structure of the idealized eastward-propagating delayed oscillator mode. (a) SST anomalies, (b) thermocline depth anomalies. Gray shading indicates warm anomalies and deeper thermocline. $H = 115$ m, $\tau = 1$, $\Delta T = 7^{\circ}\text{C}$. The structure of the mode is very similar to that of the mode at point D in Fig. 4.

ues of the parameters H and τ is shown in Fig. 4. The value of ΔT is held fixed for the time being. Figure 4c shows the temperature of the eastern equatorial Pacific in the background state (which is equivalent to showing the zonal temperature gradient at the surface since the temperature of the western Pacific remain approximately the same). A striking feature in Fig. 4b is the existence of two families of unstable modes. The one, in the neighborhood of point D, is associated with a deep thermocline and with long periods on the order of several years. The other, in the neighborhood of point E, is associated with a shallow thermocline and with short periods on the order of a year or two. We shall refer to these as the remote and local modes respectively. The first family is related to the delayed oscillator mode originally discussed by Schopf and Suarez (1988) and Battisti and Hirst (1989). The second family has some similarities with the SST modes introduced by Neelin (1991).

To analyze and categorize the modes it is convenient to focus on the processes that influence SST, the only oceanic variable with an influence on the atmosphere in this model. To that end we write the SST equation as follows:

$$\begin{aligned} T'_t + \overline{U}T'_x + U'\overline{T}_x + \overline{W}T'_z + W'\overline{T}_z \\ = -qT' + \nu T'_{xx} \end{aligned} \quad (3.1)$$

where T_x and T_z are the zonal and vertical temperature gradients; U and W are the zonal and vertical velocities; and the bars and primes denote mean and anomalous values, respectively. The terms on the right-hand side of (3.1) represent the linear damping and temperature diffusion; for details see appendix A. Neither these terms, nor the mean advection of the anomalous temperature ($\overline{U}T'_x$) can produce natural modes of oscillation by themselves and are therefore of secondary importance in this analysis. They are nonetheless retained because they can affect the properties of the possible modes.

The natural modes of oscillation in the neighborhood of point D in Fig. 4 have the structure shown in Fig. 5 and are characterized by a dominance of the term $\overline{W}T'_z$ in the SST equation—dominance of the mean upwelling of the anomalous vertical temperature gradient. The results for point D remain essentially the same if, in the SST equation, only $\overline{W}T'_z$ and the time-dependent term are retained on the left-hand side of (3.1). These vertical movements of the thermocline that have the dominant effect on SST are induced by the winds farther west. The period of the mode is so long that it involves the dynamical adjustment of the ocean basin to changes in the winds to the west of the SST variations. A slight lag between a change in the winds, and the response of the ocean to that change, is of central importance to this mode whose physics is clearly related to the “delayed oscillator” mode. This conclusion is corroborated by the structure in Fig. 5 that closely resembles that of the mode as simulated by Battisti and Hirst (1989) and others, and also the “recharge oscillator” mode introduced by Jin (1997a,b). Absent from Fig. 5 is explicit evidence of equatorially trapped Kelvin and Rossby waves, features that some people associate with the term delayed oscillator. However, as pointed out by Neelin et al. (1998) and others, these modes cannot reveal explicit evidence of such waves because they have such long periods that the equatorial zone of the ocean is almost in equilibrium with the winds. These modes are usually associated with the delayed oscillator equation that describes time dependence but says nothing about spatial structure. Neelin et al. (1998) point out that the derivation of this equation from the linearized equations of motion requires a number of assumptions, some of which are of questionable validity. The differentio-delay equation nonetheless provides valuable insight as regards the processes involved in this type of mode; a derivation is given in appendix B.

In Fig. 4, the black dashed line, which is the same

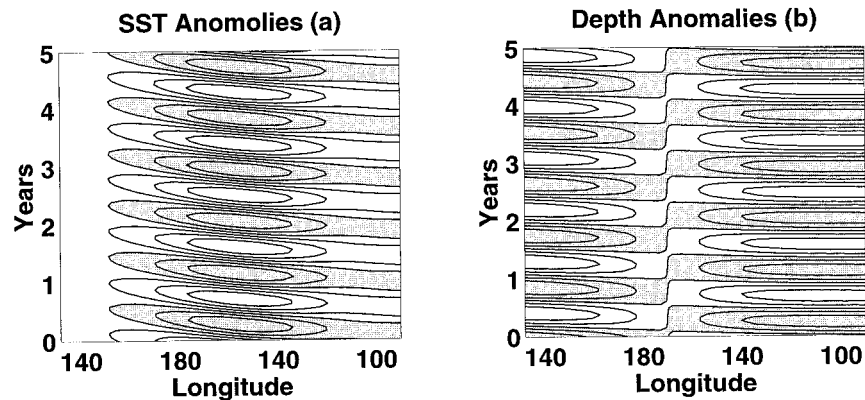


FIG. 6. The time–space structure of the idealized westward-propagating local mode. (a) SST anomalies, (b) thermocline depth anomalies. Gray shading indicates warm anomalies and deeper thermocline. $H = 115$ m, $\tau = 1$, $\Delta T = 7^{\circ}\text{C}$. The structure of the mode is very similar to that of the mode at point E in Fig. 4. For the realistic coupling strength this mode is damped.

in Figs. 4a–c, is the line of neutral stability or zero growth rate. [In the white region, the ocean–atmosphere modes lose their basin-scale spatial structure and merge with the unimportant scattering modes (see JN) that are confined to the neighborhoods of coasts.] It follows that the presence of the delayed oscillator mode requires zonal winds of a certain intensity, and a thermocline that is neither too shallow nor too deep. This last condition can easily be explained. When the thermocline is too deep, its vertical movements have little impact on SST so that ocean–atmosphere interactions are precluded. Under such conditions, an intensification of the background winds brings those interactions into play by raising the thermocline in the east while it deepens in the west. Hence the condition that the intensity of the winds exceed a certain value. A shoaling of the thermocline—a movement to the left of point D in Fig. 4—stabilizes the delayed oscillator mode because a decrease in the value of H lowers the mean surface temperature in the east (as can be seen in Fig. 4c) thus reducing vertical temperature gradients. Such a shoaling has another effect, however; it increases zonal temperature gradients, bringing into play a different type of instability.

In the vicinity of point E in Fig. 4, SST variations depend mainly not on vertical movements of the thermocline, but on the anomalous advection of the mean zonal temperature gradient $U'\overline{T}_x$ and on the anomalous upwelling of the mean temperature gradient $W'\overline{T}_z$, that is, on “local” effects. Figure 6 depicts the time–space structure of the mode when only the terms $U'\overline{T}_x$ and $W'\overline{T}_z$ are retained in Eq. (3.1). It is essentially the same as the structure of the modes at point E. In contrast to modes that involve mainly \overline{WT}'_z , those in Fig. 6 have relatively short periods, and are associated with the westward phase propagation of SST anomalies.

In a series of publications Neelin (1991), Jin and Neelin (1993), Neelin et al. (1994), and Neelin et al. (1998) discussed two useful limits for considering the dynamics

of the ocean–atmosphere—the so-called fast wave and fast SST limits. The distinction between them is based on the different timescales of SST and ocean evolutions in the coupled system. In the fast wave limit the adjustment of the ocean is instantaneous, so that the terms associated with the time derivatives in the shallow-water equations can be dropped. The local modes in the vicinity of point E appear to have much in common with the westward-propagating modes in the fast wave limit (see Jin and Neelin 1993). In the fast SST limit, changes in SST are instantaneous. Temporal dependence is therefore unimportant in the SST equation, but allows for a time delay between wind fluctuations and the subsequent ocean adjustment. This explains certain similarities between the modes in the vicinity of point D and some of the modes in fast SST limit.

Difficulties in establishing a close correspondence between the modes described here and those discussed in the above papers arise for the following reasons. The fast wave limit corresponds to a large value for c , the Kelvin wave speed, the fast SST limit to a low value for c . (Jin and Neelin express these limits in terms of nondimensional numbers.) In the terminology of this paper, the value of c can be changed by altering the depth of the thermocline H . Increasing H should move us in the direction of the fast wave limit, but the results in Fig. 4 indicate the very opposite. This happens because a deeper thermocline affects not only the wave speed but also the coupling between the ocean and the atmosphere: the deeper the thermocline, the smaller the direct effect the wind has on SST variations. The latter tendency favors the remote mode (or fast SST limit), to an even greater degree than effects associated with changes in the speed of Kelvin waves. Hence the difficulty in relating the results presented here to those of Jin and Neelin is the lack of a one-to-one correspondence between our parameters (H , etc.) and their nondimensional parameters. A change in the value of any one of our parameters corresponds to changes in several

TABLE 1. Different modes of oscillation and their properties.

Mode type	SST equation terms	Effects	Propagation of SST and wind anomalies	Period	Associated with
Local	$U'\bar{T}_x + W'\bar{T}_z$	Zonal advection, entrainment across the thermocline	Westward	8–14 months	Annual cycle
Remote (delayed oscillator)	$\bar{W}T'_z$	Vertical movements of the thermocline	Slightly eastward	3–10 yr	El Niño

of their parameters, or vice versa. The advantage of classifying the modes according to dimensional parameters such as H , τ , and ΔT , and the processes that determine SST variations, become apparent in a discussion of measurements in the next section.

In summary, a stability analysis indicates two families of unstable modes to which we refer as local and “remote” modes because SST variations depend on upwelling and advection induced by local wind fluctuations (close to the SST variations) in the one case, and in the other case depend on vertical movements of the thermocline in response to wind fluctuations farther west. The differences between the two families of

modes, listed in Table 1 and depicted schematically in Figs. 7 and 8, are most pronounced if we compare a mode at point D with one at point E in Fig. 4. At other points on the dispersion diagram the modes are of a hybrid character, with aspects of both families, to a degree that depends on the proximity of a mode to either points E or D. We discuss this matter in the next section.

Why does a deeper thermocline favor the remote mode? The reason is simple—if the thermocline is relatively deep then both the mean vertical \bar{T}_z and zonal \bar{T}_x temperature gradients near the surface are too weak so that the term $\bar{W}T'_z$ becomes dominant. Similarly, for moderate values of H (in the middle of the stability diagram) a weakening of the mean wind deepens the thermocline in the east and hence results in the intensification of the remote mode at the expense of the local

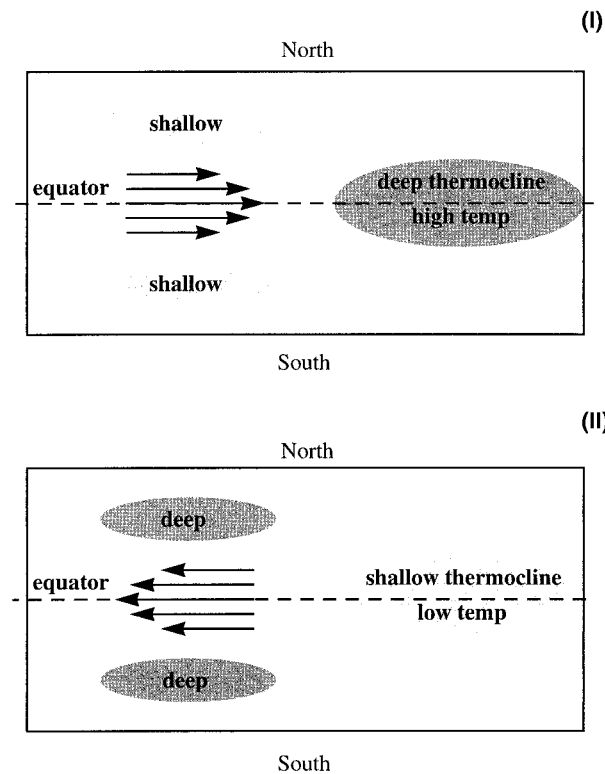


FIG. 7. A schematic diagram that shows the spatial (lat–long) structure of the delayed oscillator or remote mode (corresponding to point D in Fig. 4). Arrows indicate winds, shaded areas changes in thermocline depth, and temp refers to temperature. (These are all departures from a background state.) This mode, referred to as the delayed oscillator, is associated with a deep thermocline. The sketch shows conditions during El Niño (I) and La Niña (II).

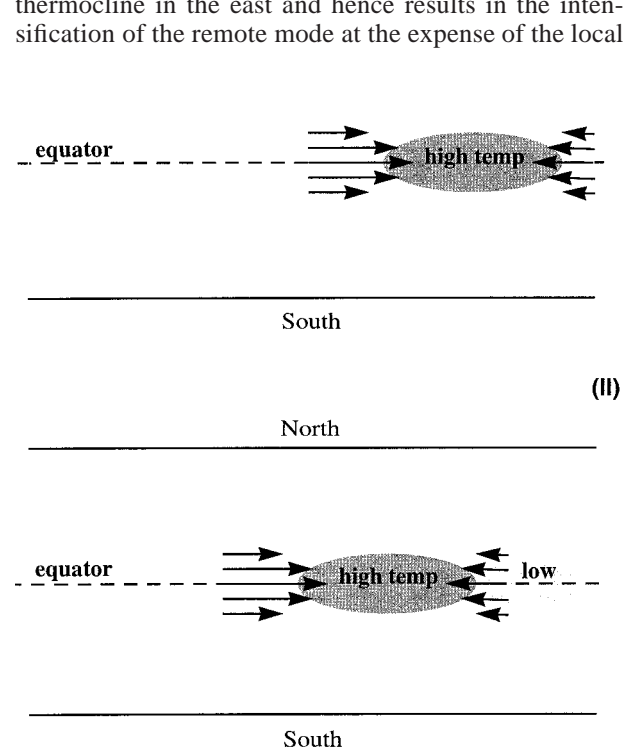


FIG. 8. A schematic diagram that shows the spatial (lat–long) structure of the local mode (corresponding to point E in Fig. 4). Arrows indicate winds, shaded areas changes in SST, and temp refers to temperature. (These are all departures from a background state.) This mode has a relatively short period of a year or two and is associated with a shallow thermocline and the westward propagation of SST anomalies. The sketch shows conditions during the warm (I) and transitional phases (II).

mode, which again leads to the oscillation with longer periods.

4. A discussion of measurements

The Southern Oscillation, as observed since the 1980s, corresponds to a mode in the vicinity of point A in Fig. 4 and hence is a hybrid mode in which several physical processes influence SST variations. This is consistent with various observers who point out that the delayed oscillator mode fails to account for a number of aspects of the Southern Oscillation in reality. That mode is a considerable part of the story, however, because its “memory”—the process mainly responsible for it being continual—is in the form of subsurface undulations of the thermocline which, in the eastern equatorial Pacific, exert a strong influence on SST.

To capture conditions during the 1960s and 1970s when time-averaged surface temperatures in the eastern Pacific Ocean were lower (corresponding to the more intense zonal winds) requires movement from point A toward B. Local processes now have a stronger influence on SST so that the mode acquires features resembling those in Fig. 6, and tends to have westward phase propagation. Figure 9 shows this change in the period and structure of the mode associated with a move from point A to B to C in Fig. 4. In their review of El Niño episodes up to and including 1976, Rasmusson and Carpenter (1982) emphasize westward phase propagation along the equator, in sharp contrast to what happened in 1982 when El Niño evolved in an eastward direction (Rasmusson and Wallace 1983). This difference is clearly evident in the two panels of Figure 10. A change in the background conditions—the move from A to B—appears to have contributed to that change in the properties of El Niño before and after the late 1970s.

The annual cycle in the eastern equatorial Pacific Ocean involves entrainment across the thermocline rather than vertical movements of thermocline (McPhaden et al. 1998), and is characterized by westward phase propagation, all features of local rather than delayed oscillator modes. A local mode is dominant for parameters in the vicinity of point E in Fig. 4, but for parameters that correspond to conditions today, such modes are damped. Some of their properties nonetheless manifest because there is forcing at the right (relatively short) period of 1 yr.

If parameters should change so as to favor the dominance of local processes and modes with a short period, then interactions between the seasonal cycle and the natural modes could become strong. Consider, for example, a move that lowers temperatures, and intensifies the winds thus promoting the influence of zonal advection of surface waters on SST—a move toward point C with the characteristic period between 1 and 2 yr. Figure 9c shows the structure at point C. Such conditions, which favor a weaker interannual but enhanced annual signal, could have prevailed from the 1940s to the late

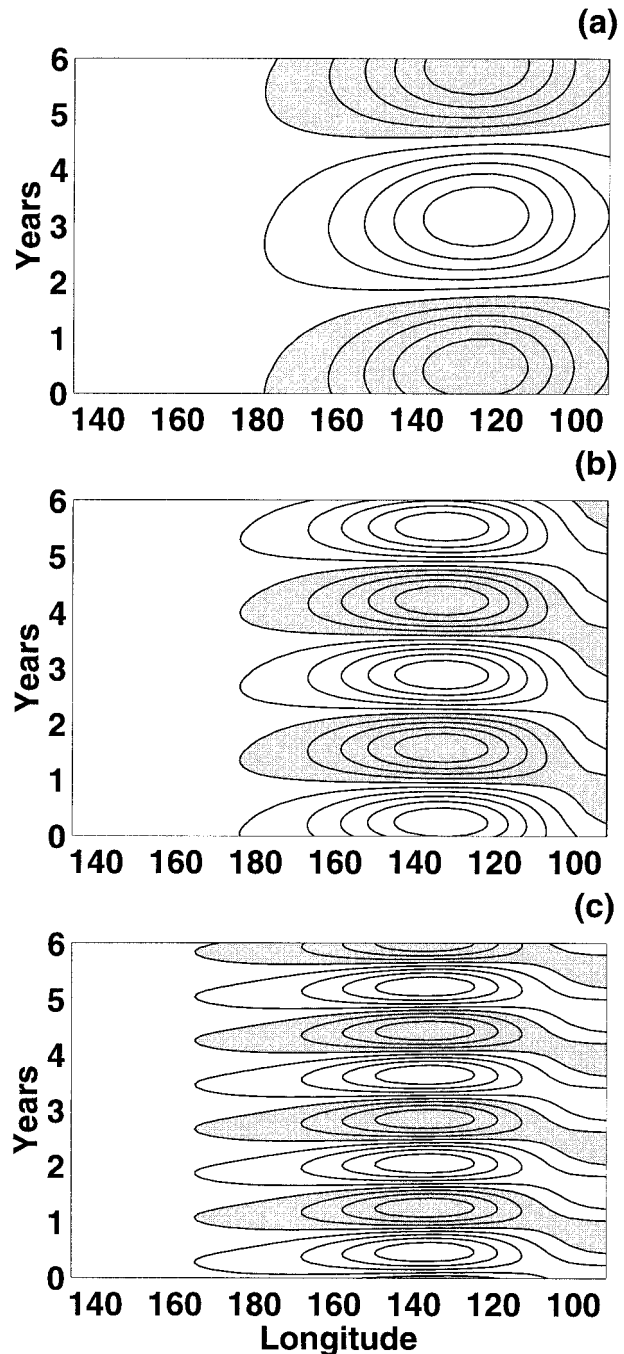


FIG. 9. The time–space structure of the hybrid modes at points A, B, and C in Fig. 4 as manifested in the anomalous SST as a function of long and time. (a) For point A, a lower-frequency (5-yr period) mode with a slight eastward propagation and the properties of the delayed oscillator dominant; (b) for point B, a higher-frequency (approximately 3-yr period) mode with a dominant westward propagation; (c) for point C, a high-frequency (1–2-yr period) mode.

1950s. A wavelet spectral analysis of the unfiltered temperature record in Fig. 2 shows a strong annual cycle and very few El Niño episodes during that period. The low correlation between the Southern Oscillation index

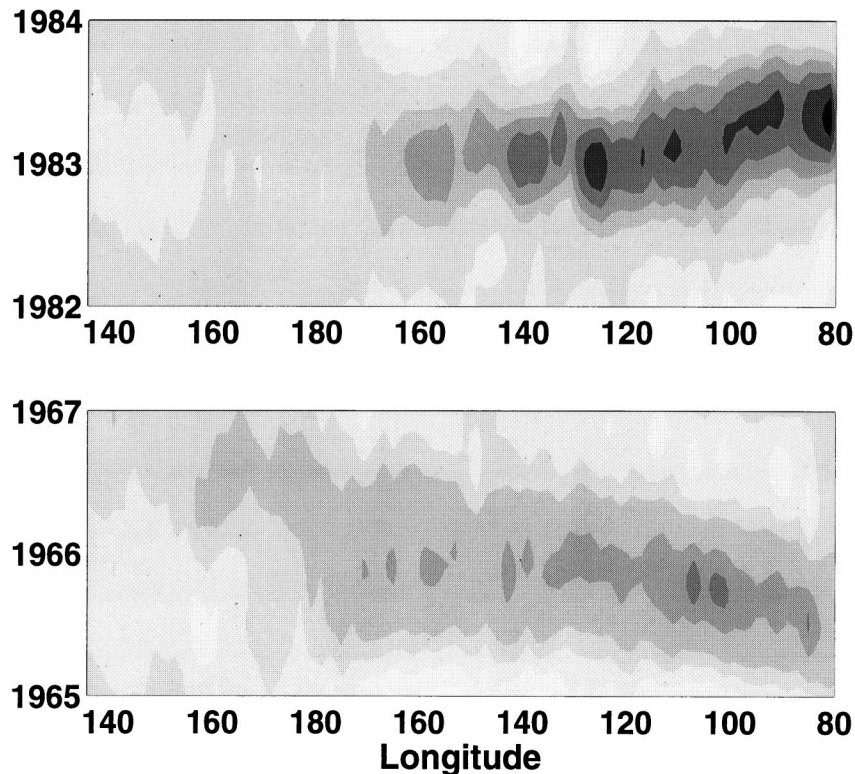


FIG. 10. El Niño of 1982/83 and 1965/66 revealed in SST along the equator as a function of time, after subtraction of the decadal fluctuation. The difference in the direction of phase propagation is evident. Darker shading corresponds to warm SST anomalies. The time axis starts on 1 Jan in each panel.

(SOI; showing the pressure difference across the Pacific basin) and the SST of the eastern Pacific during that period is also consistent with a dominance of local processes associated with advection and changes in upwelling over remote processes associated with the delayed oscillator. The link between the eastern and western regions of the Pacific ocean through the delayed oscillator mechanism was temporarily lost, which was reflected in the low SOI and its low correlation with SSTs. An additional factor that may have contributed to the absence of interannual El Niño episodes was the availability of only strongly damped modes in the neighborhood of point C.

For very strong winds and zonal temperature gradients, a move toward point E, the dominant mode has a short period (close to 1 yr) so that the annual cycle is likely to be far more prominent than any interannual variability. It will be a valuable check on the theory presented here to determine whether those were the conditions during the last glacial maximum, some 20 000 yr ago when the winds were intense (Fairbanks 1989; Schrag et al. 1996; Andreason and Ravelo 1997).

Deposits in a lake in southwestern Ecuador indicate that whereas El Niño today occurs every 3–5 yr, the interval between successive events was far longer, on the order of a decade, some 7000 yr ago (Rodbell et al.

1999). Information about the background state at that time is contradictory. Geoarchaeological data suggest that the eastern equatorial Pacific was warm (Sandweiss et al. 1996), but other sources indicate that the coastal zone of Peru was arid so that the adjacent ocean must have been cool (Wells and Noller 1997). The results in Fig. 4 favor the latter state of affairs because, for the Southern Oscillation to have a very long period requires a move in the direction of point D—a large value for H and intense winds that cause a shallow thermocline and low SST in the east. The measurements indicate that the period of the Southern Oscillation was very long some 7000 yr ago, but then gradually decreased. This suggests a move from point D toward A—a gradual weakening of the winds and shoaling of the thermocline. Another possibility is that the thermocline was so deep sometime in the past that the Southern Oscillation was absent. Figure 4 implies that a gradual shoaling of the thermocline would then have led to the emergence of an oscillation with relatively long periods at first, then with progressively shorter periods as the thermocline continued to shoal.

5. Stability properties: Changing ΔT

In section 4 the temperature difference across the thermocline ΔT was constant; now we study the effects of

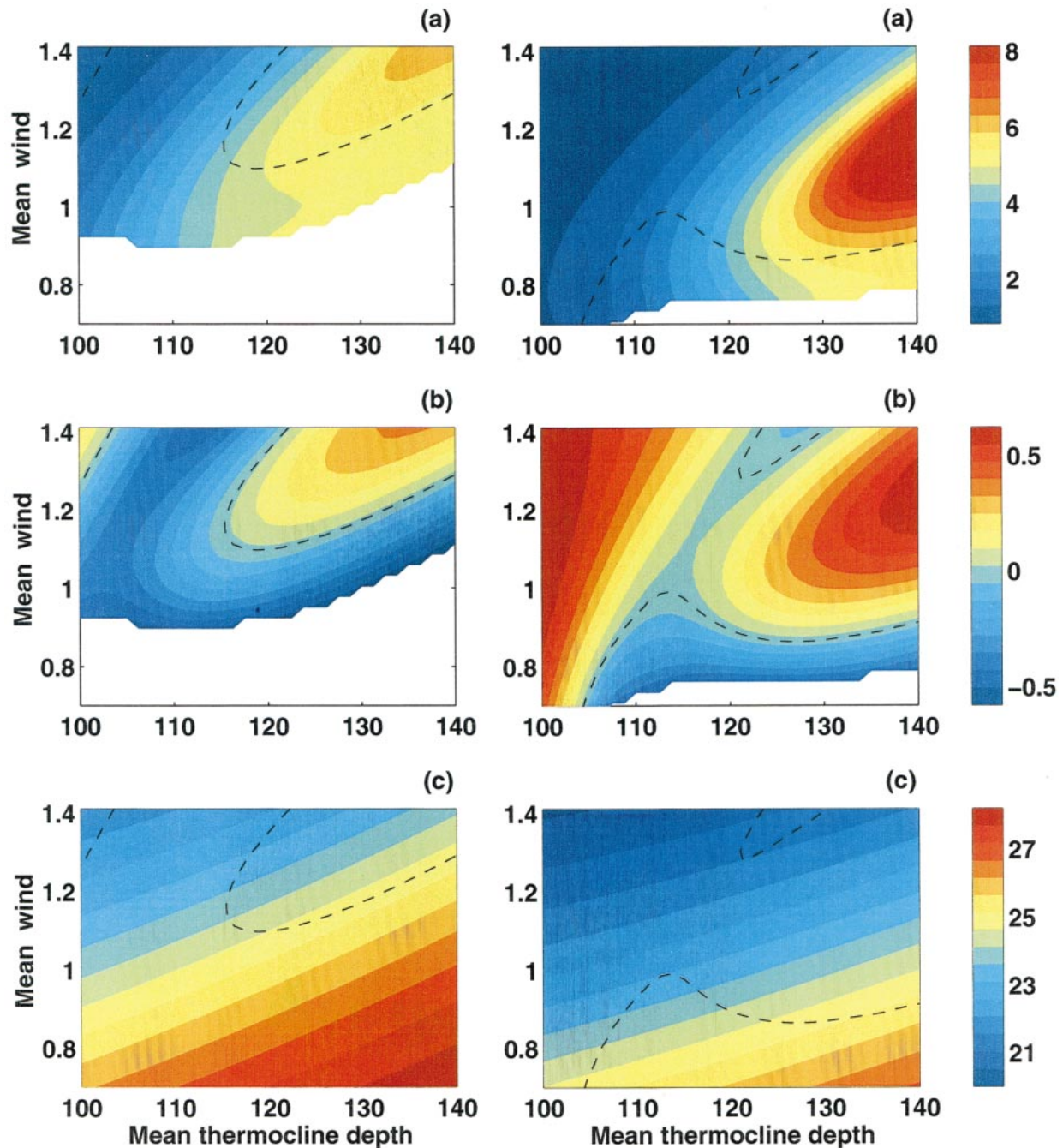


FIG. 11. Changes in (a) the period and (b) growth rates of the most unstable oscillations as a function of changes in the easterly winds along the equator, and in the depth of the equatorial thermocline (in meters). (c) The minimum SST (in $^{\circ}\text{C}$) of the basic state in the eastern Pacific Ocean. The value of ΔT measured over a 50-m depth variation is 8°C for the left-hand panels and 6°C for the right-hand panels (cf. Fig. 4 with $\Delta T = 7^{\circ}\text{C}$). $H = 120$ m. The dotted line corresponds to the line of zero growth rate; in the white area both amplifying and damped modes are absent. To keep the same color map in panels (a) all periods from 8 to 12 yr are shown with the same color (dark red).

changing this parameter on the stability properties. The results in Fig. 11 are similar to those in Fig. 4 except that, in the left-hand panels the value of ΔT is 1°C higher, while it is 1°C lower in the right-hand panels than for Fig. 4. An increase in ΔT is stabilizing because it inhibits entrainment across the thermocline, and also

the vertical movements of the thermocline. (Increasing ΔT results in a sharper thermocline, with a weaker slope. This implies a larger T_z at the thermocline, but reduced T_z at the base of the mixed layer from where the water is entrained, and, consequently, a warmer eastern equatorial Pacific, evident in the lowest panels of Fig. 11.)

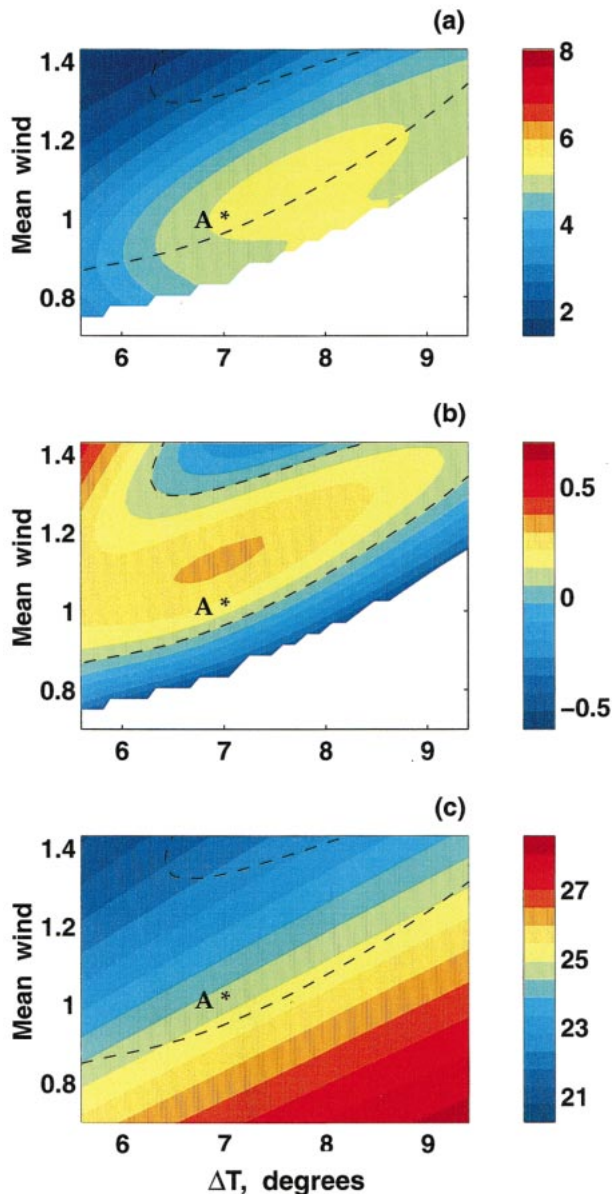


FIG. 12. Changes in (a) the period and (b) growth rates of the most unstable oscillations as a function of changes in the easterly winds along the equator, and in the temperature difference across the thermocline ΔT (in $^{\circ}\text{C}$). The value ΔT is measured over a 50-m depth variation. $H = 120$ m. The dotted line corresponds to the line of zero growth rate; in the white area both amplifying and damped modes are absent. (c) The minimum SST (in $^{\circ}\text{C}$) of the basic state in the eastern Pacific Ocean. Point A corresponds to the present condition in the Tropics.

These stabilizing changes in the background state cause the regions of instability in the left-hand panels of Fig. 11 to shrink (in comparison with those in Fig. 4) and cause the white region (where no modes are present) to expand. Decreasing the value of ΔT has the opposite effect. (See the right-hand panels of Fig. 11.)

Next the depth of the thermocline H is left unchanged while the values of τ and ΔT are varied. Figure 12

confirms that an increase in the temperature difference ΔT has a stabilizing effect on the oscillations—if ΔT is too large there are no unstable modes (white area of the Fig. 12)—and tends to lengthen the period of the oscillation. The modes are amplifying between the dashed lines (i.e., between the neutral stability lines) and decaying in the rest of the stability diagram. Comparing Figs. 4 and 12 also suggests that, for the hybrid modes in the middle of the stability diagrams, there may exist the optimal intensity of the mean wind (corresponding to the optimal thermocline slope) that results in the maximum growth rates of the Southern Oscillation. On the other hand, the local minimum of instability for stronger winds evident in Fig. 12 is related to a separation of the remote (in the middle of the diagram) and local (in the upper left-side corner of the diagram) modes for different ΔT .

Note that some nonlinear numerical models show a general increase of interannual variability when ΔT increases (e.g., Munnich et al. 1991). There are two possible explanations for such behavior. The first possibility, consistent with the analysis in Fig. 12, would suggest that those models may simulate mean states that are positioned on the stability diagram to the left from one of the instability maxima ($\tau \sim 1.1$, $\Delta T \sim 6^{\circ}\text{--}7^{\circ}$). The second possibility is purely nonlinear: for large ΔT even relatively small perturbations in the system can change the temperature of the entrained water much more efficiently than a linear model would assume. The extent to which such nonlinearity can be important is related to the same question—how far away from the neutral stability the mean state is.

6. Conclusions

Ocean–atmosphere interactions in the Tropics give rise mainly to two types of modes: low-frequency, delayed oscillator modes in which SST variations depend mainly on vertical movements of the thermocline that form part of the basinwide oceanic adjustment to changes in the winds; high-frequency, local modes in which SST changes depend on wind-induced upwelling and advection. The first type is favored when the thermocline is deep, the latter when it is shallow. Both require zonal winds of a certain intensity, to elevate the thermocline in the east in the case of the delayed oscillator, and to create zonal temperature gradients in the case of the local modes. The observed Southern Oscillation is a hybrid mode whose properties change gradually with time as the background state changes. For example, a deepening of the thermocline suppresses the local processes in favor of “remote-controlled” processes so that the delayed oscillator mode becomes dominant, causing the period of the Southern Oscillation to increase. An increase in ΔT is stabilizing.

These results have important implications for the debate about the interpretation of the temperature record in Fig. 1. The debate is really about two separate but

related issues, the decadal fluctuation, and the interannual variability. If the first is a reality determined by physical processes distinct from those of the Southern Oscillation, then it should affect the properties of that oscillation. We do indeed find that the changes in the properties of El Niño from the 1960s to the 1990s (the period of the Southern Oscillation increased from approximately 3 to 5 yr; the structure of the oscillation changed, etc.) are consistent with the presence of a decadal fluctuation that was observed to deepen the thermocline in the eastern tropical Pacific, and to weaken the trade winds. The origin of the decadal oscillation, and whether global warming is affecting it, are at this time unclear. Furthermore, any one change in the properties of El Niño, the decrease in its frequency of occurrence say, can not be confirmed by means of standard spectral analyses because there are too few realizations of El Niño before the decadal fluctuation alters background conditions. There is nonetheless reason to believe that the properties of the Southern Oscillation have been changing gradually as part of a decadal modulation, because the indications of different changes in the properties of El Niño are all consistent with each other.

Despite the simplicity (crudeness) of our model, it offers explanations for a number of phenomena, and can provide a rough guide to the interpretation of measurements and model results. Values for H and ΔT can readily be assigned in the case of oceanic models with only two layers, or a relatively sharp thermocline. However, multilayer models are more problematic, especially if the thermocline is diffuse. This is a factor in attempts to explain why different global climate models—those of Tett (1995) and Meehl et al. (1993) for example—give different results as regards the impact of global warming on El Niño. Those models tend to simulate Southern Oscillations that differ significantly from the one observed over the past few decades, presumably because the models do not capture conditions in the vicinity of points A and B in Fig. 4. For example, in the most recent calculation (Timmerman et al. 1999), in which the oceanic component of the model has a high resolution, the Southern Oscillation is too regular and has too short a period—the model appears to capture conditions somewhere between points B and C in Fig. 4, those associated with a period of about 2 yr and with too strong a cold tongue in the eastern and central Pacific Ocean. Once a model reproduces the conditions of today, it next has to simulate how global warming will alter the background state. On this matter the models disagree; some indicate a warming, some a cooling of the eastern tropical Pacific. The situation is further complicated by the fact that H and ΔT can change simultaneously with either reinforcing or counterbalancing effects. Clarification of these issues, which will help determine whether the warming of the eastern tropical Pacific during the 1980s and 1990s is a manifestation of global warming, will have to wait until we understand better the decadal variability.

This paper concerns changes in the properties of El Niño in response to gradual changes in the background state. In reality, each El Niño is distinct and, as the events of 1992 and 1997 demonstrated, can be enormously different from others. Of the various processes neglected in this paper, westerly wind bursts are particularly likely to contribute significantly to the differences between one El Niño and the next. (See, e.g., McPhaden et al. 1998.) Because those winds are confined to the neighborhood of the date line, they are likely to affect developments farther east by their effect on vertical movements of the thermocline. This means that their influence should be prominent when modes of the delayed oscillator type are favored. That has been the case since the 1980s. Since that time, a Southern Oscillation, with a period close to 5 yr, appears to have been present continually. If so, then the phase of that oscillation determined the impact of westerly winds bursts at different times (in the same way that the phase of a swinging pendulum determines the impact of random blows always in the same direction). This interplay between the natural mode of oscillation and random wind disturbances will be explored on another occasion (Fedorov 2001).

Acknowledgments. We thank P. Chang, S. Griffies, S. Harper, M. Harrison, M. McPhaden, M. Latif, D. Neelin, A. Rosati, E. Tziperman, B. Winter, and A. Wittenberg for valuable discussions and comments. This research was supported by NOAA under Contract NA86GP0338.

APPENDIX A

The Model Equations

The ocean dynamics in the model is described by the linear shallow-water equations on the equatorial β -plane in the long-wave approximation. For simplicity, symmetry with respect to the equator, and no annual forcing are assumed:

$$u_t + g'h_x - \beta yv = \hat{\tau}/\rho d - ru \quad (\text{A.1})$$

$$h_t + H(u_x + v_y) = -rh, \quad (\text{A.2})$$

$$g'h_y + \beta yu = 0. \quad (\text{A.3})$$

The notation is conventional with positive $h(x, y, t)$ denoting the total local depth of the thermocline, $u(x, y, t)$ the zonal velocity, $v(x, y, t)$ the meridional velocity, $\hat{\tau}(x, y, t)$ the zonal wind stress, d the depth characterizing the effect of wind on the thermocline, ρ the mean water density, r the linear Raleigh damping, H —the mean depth of the thermocline and g' the reduced gravity, which depends linearly on the vertical temperature gradient $\Delta T_1/\Delta z_1$ measured at the thermocline, that is,

$$g' = \Gamma \Delta T_1/\Delta z_1, \quad (\text{A.4})$$

where Γ is the coefficient of proportionality, and ΔT_1 and Δz_1 will be specified later—see (A.13).

The standard no-flow boundary condition is applied at the eastern ocean boundary ($x = x_E$), and the no-net-flow condition at the western boundary ($x = x_W = x_E - L$), where L is the length of the basin. The shallow-water equations are integrated by applying the method of characteristics similar to that of Battisti (1988). We expand the solutions into a Kelvin wave and a set of Rossby waves, using the first 11 symmetric Rossby waves. The finite differencing of the equations is done on a 30-point grid in the x direction with the grid resolution/time step ratio equal to the linear Kelvin wave speed c ,

$$c = (Hg')^{1/2}. \tag{A.5}$$

An embedded mixed layer of the thickness d^s with the linear damping r^s allows for a shear near the surface by introducing additional surface flow (u^s, v^s):

$$r^s u^s - \beta y v^s = \hat{\tau} / \rho d^s, \tag{A.6}$$

$$r^s v^s + \beta y u^s = 0. \tag{A.7}$$

The full zonal velocity U at the surface and the vertical velocity W at the base of the mixed layer are

$$U = u + u^s, \tag{A.8}$$

$$W = w + w^s \tag{A.9}$$

with

$$w = -h_t \frac{d^s}{H}. \tag{A.10}$$

The dynamics of the SST in the equatorial strip is approximated by the parameterized advection–diffusion equation:

$$T_t + UT_x + WT_z = \nu T_{xx} - q(T - T^q), \tag{A.11}$$

where the sea surface temperature $T = T(x, t)$ is measured at the equator. All the processes responsible for the warming of the surface are combined and described by a linear term in (A.11), which restores the temperature to some warm equilibrium temperature T^q .

The vertical upwelling term WT_z is estimated as

$$WT_z = \gamma \Theta(W) W \frac{T - T^e}{d^s}, \tag{A.12}$$

where $\Theta(W)$ is the theta function (reflecting the fact that downwelling cannot change the temperature at the surface), and γ is the effectiveness of the upwelling.

The entrainment temperature T^e at the base of the mixed layer is calculated as

$$T^e = T^o + \begin{cases} \Delta T_1 \tanh[(h - d^s)/\Delta z_1], & h > d^s \\ \Delta T_2 \tanh[(h - d^s)/\Delta z_2], & h < d^s. \end{cases} \tag{A.13}$$

This parameterization describes the temperature field with a tanh-like structure centered at the thermocline that corresponds to the T^o isotherm. Importantly, when

the thermocline is deep (H and therefore h large) $T^e \approx T^o + \Delta T_1$. When the thermocline is shallow (H and therefore h small) $T^e \approx T^o - \Delta T_2$. To keep a continuous first derivative at $h = d^s$ we choose

$$\Delta T_2 = k \Delta T_1 \quad \text{and} \quad \Delta z_2 = k \Delta z_1, \tag{A.14}$$

where k is some factor, so that

$$\Delta T_1 / \Delta z_1 = \Delta T_2 / \Delta z_2. \tag{A.15}$$

The characteristic temperature across the thermocline (ΔT) used in text of the paper is, in fact, proportional to the temperature gradient across the thermocline $\Delta T_1 / \Delta z_1$, and, if measured over a 50-m depth difference, is calculated as

$$\Delta T = (\Delta T_1 / \Delta z_1) \times 50 \text{ m}. \tag{A.16}$$

To change ΔT we actually vary Δz_1 .

Similar to the approach by JN the wind stress is split into the mean part τ and the perturbation τ' :

$$\hat{\tau} = \bar{\tau} + \tau', \tag{A.17}$$

with

$$\bar{\tau} = \tau P \cdot F(x) \exp(-\alpha y^2 / 2), \quad \text{and} \tag{A.18}$$

$$F(x) = 0.01 - \cos^2(p(x - x_o) / L), \tag{A.19}$$

where $F(x)$ approximates the shape of the zonal mean wind at the equator, P is a dimensional amplitude, and τ is the nondimensional wind strength. Throughout our calculations the shape of the wind stress remains fixed, but τ changes. The meridional structure of both the mean and perturbation winds is assumed to be Gaussian with the ratio between the oceanic and atmospheric Rossby radii of deformation equal to $\alpha^{1/2}$.

The perturbation part of the zonal wind stress is related to the SST anomaly $T' = T'(x, t)$ through the simplified Gill-type atmospheres (for details see JN):

$$\begin{aligned} \tau' = & \mu \lambda A \exp(-\alpha y^2 / 2) \\ & \times \left[\frac{3}{2} \exp\left(\frac{3 \varepsilon x}{L}\right) \int_x^{x_E} T' \exp\left(-\frac{3 \varepsilon x}{L}\right) \frac{dx}{L} \right. \\ & \left. - \frac{1}{2} \exp\left(-\frac{\varepsilon x}{L}\right) \int_{x_W}^x T' \exp\left(\frac{\varepsilon x}{L}\right) \frac{dx}{L} \right], \end{aligned} \tag{A.20}$$

where M is a dimensional amplitude and μ is the non-dimensional coupling strength, and λ is a spatially varying factor.

In contrast to JN work, in our study the non-dimensional inverse atmospheric damping scale ε varies with longitude:

$$\varepsilon = \varepsilon_o \left[1 + \eta \exp\left(-3 \frac{(x - x_w)^2}{L^2}\right) \right]. \tag{A.21}$$

For positive η the damping is larger near the western boundaries, and smaller in the eastern Pacific. Such dependence prevents the winds from spreading beyond the

TABLE A1. The list of parameters used for calculations.

Variable	Value	Variable	Value
L	145°	x_w	130°E
d	75 m	d^s	50 m
ΔT_1	10°C	k	1.5
T°	20°C	T^q	29.5°C
γ	0.5	Γ	0.37 m ² s ⁻² K ⁻¹
q^{-1}	125 day	r^{-1}	2.5 yr
x_o	215°	p	2.7
P	0.07 Pa K ⁻¹	A	0.04 Pa K ⁻¹
ϵ_o	1	α	0.07
η	1	μ	0.9
v	10 ⁵ m ² s ⁻¹	$(r^s)^{-1}$	1.5 day

western boundary. This also allows us to change the properties of the atmosphere to achieve a more realistic response of the atmosphere to a given SST.

Finally, since the Gill atmosphere tends to give too strong winds near the eastern boundary, another modification is made to the winds, such that τ' given by (A.20) is multiplied by a spatially varying factor λ :

$$\lambda = \lambda(x) = 0.5 \langle \tanh[10(x - x_E)/L] + 1 \rangle. \quad (\text{A.22})$$

The factor λ is equal to unity almost everywhere in the basin but approaches 0.5 near the eastern boundary, reducing the wind perturbation there. This modification is important but does not affect our solutions qualitatively.

Although the model is inspired by the “strip-down” model by JN, important differences with the JN model include the following.

1) The ocean:

To ensure the necessary sensitivity of the thermocline to changes in the winds, the depth scale d characterizing the effect of wind on the thermocline is chosen to be different from the mean depth of the thermocline (approximately 1.5 times smaller).

2) The model atmosphere:

The atmospheric damping scale $\epsilon(x)$ varies with longitude. An additional scaling factor $\lambda(x)$ is used to reduce winds near the eastern boundary.

3) The SSTs:

The SST equation has a second-order zonal diffusion, and no meridional terms. The tanh functions in the parameterization of the entrainment temperature are different above and below the thermocline, ensuring that T^e better matches the actual subsurface temperature distribution in the equatorial Pacific Ocean. Also, the effectiveness of upwelling γ is slightly smaller in our approach than in JN.

The model is run with the parameters given in Table A1. In addition, H , τ and ΔT must be specified.

Of the other various parameters that determine the properties of the simulated Southern Oscillation, the one with a particularly strong influence is the coupling strength μ of the atmospheric response to a given SST. Increasing the value of this parameter usually increases

both the growth rates and the periods of oscillations. Above a certain threshold, the unstable solution may cease to be oscillatory, and become exponentially growing—in terms of JN, the solution may merge with the strongly growing stationary mode.

Although changing μ is convenient in studies of the properties of the modes in simple models, in realistic GCMs the coupling strength is not an adjustable parameter. Nor is it a parameter that can be measured from observations in a straightforward manner. That is another reason why we fix μ at some reasonable value and study properties of the system for different H , τ , and ΔT .

The atmospheric damping scale ϵ also influences the structure of the modes because it determines the location of the maximum response of the winds to a given SST. For example, the winds in response to a SST anomaly in the eastern Pacific have a maximum near the date line for a small value of ϵ but, as that value increases, the maximum winds shift eastward. Hence the winds for small ϵ affect the SST mainly by altering the depth of the thermocline in the east but, in the case of large ϵ , affect SST by changing local upwelling. Hence, a change in the properties of the atmospheric model can shift solutions from a remote mode to the local mode. In addition, any change in the structure of the mean wind [given by $F(x)$], especially in the eastern Pacific, is likely to affect the structure of the dominant mode of oscillation.

APPENDIX B

The Delayed Oscillator Equation

The delayed oscillator equation can be deduced by using the main temperature balance for the mode at point D in Fig. 4

$$T'_t = -\overline{W}T'_z \quad (\text{B.1})$$

(hereafter, all variables are averaged over some domain of the eastern equatorial Pacific). We next approximate the vertical temperature gradient by the differencing

$$T'_z \sim (T' - T^{e'})/d^s, \quad (\text{B.2})$$

where T^e is the entrainment temperature at the base of the mixed layer d^s . Here $T^{e'}$ is proportional to the displacement of the thermocline h' , that is

$$T^{e'} \sim h'. \quad (\text{B.3})$$

The thermocline depth anomalies in the eastern Pacific are proportional to the zonally averaged wind anomalies at some previous moment in time ($t - \Delta t$) and, hence, proportional to T' at the time $t - \Delta t$, that is,

$$h' \sim b_1 T'(t - \Delta t), \quad (\text{B.4})$$

where Δt is the time delay due to the ocean dynamical adjustment, and b_1 is a constant. Substituting (B.2)–(B.4) into (B.1) gives

$$T'_i = aT' + bT'(t - \Delta t), \quad (\text{B.5})$$

the very differentio-delay equation that describes the linear evolution of the temperature anomalies, with some constant parameters a , b (related to d^s , b_1 , etc.) and the time delay Δt , which originally led to the term delayed oscillator.

REFERENCES

- Andreason, D. J., and A. C. Ravelo, 1997: Tropical Pacific Ocean thermocline depth reconstructions for the last glacial maximum. *Paleoceanography*, **12**, 395–413.
- Battisti, D. S., 1988: Dynamics and thermodynamics of a warming event in a coupled tropical atmosphere–ocean model. *J. Atmos. Sci.*, **45**, 2889–2919.
- , and A. C. Hirst, 1989: Interannual variability in a tropical atmosphere ocean model—Influence of the basic state, ocean geometry and nonlinearity. *J. Atmos. Sci.*, **46**, 1687–1712.
- Chao, Y., X. Li, M. Ghil, and J. C. McWilliams, 2000: Pacific interdecadal variability in this century's sea surface temperatures. *Geophys. Res. Lett.*, **27**, 2261–2264.
- Dijkstra, H. A., and J. D. Neelin, 1995: Ocean–atmosphere interaction and the tropical climatology. Part I: The dangers of flux correction. *J. Climate*, **8**, 1343–1359.
- , and —, 1999: Coupled processes and the tropical climatology. Part III: Instabilities of the fully coupled climatology. *J. Climate*, **12**, 1630–1643.
- Fairbanks, R. G., 1989: A 17000-year glacio-eustatic sea level record: Influence of glacial melting rates on the Younger Dryas event and deep-ocean circulation. *Nature*, **342**, 637–642.
- Fedorov, A. V., 2001: The response of the coupled tropical ocean–atmosphere to westerly wind bursts. *Quart. J. Roy. Meteor. Soc.*, in press.
- , and S. G. H. Philander, 2000: Is El Niño changing? *Science*, **288**, 1997–2002.
- Giese, B. S., and J. A. Carton, 1999: Interannual and decadal variability in the tropical and midlatitude Pacific Ocean. *J. Climate*, **12**, 3402–3418.
- Gu, D. F., and S. G. H. Philander, 1997: Interdecadal climate fluctuations that depend on exchanges between the tropics and extratropics. *Science*, **275**, 805–807.
- Guilderson, T. P., and D. P. Schrag, 1998: Abrupt shift in subsurface temperatures in the Tropical Pacific associated with changes in El Niño. *Science*, **281**, 240–243.
- Harrison, D. E., and N. K. Larkin, 1997: Darwin sea level pressure, 1876–1996: Evidence for climate change? *Geophys. Res. Lett.*, **24**, 1775–1782.
- Jin, F. F., 1997a: An equatorial ocean recharge paradigm for ENSO. Part I: Conceptual model. *J. Atmos. Sci.*, **54**, 811–829.
- , 1997b: An equatorial ocean recharge paradigm for ENSO. Part II: A stripped-down coupled model. *J. Atmos. Sci.*, **54**, 830–847.
- , and J. D. Neelin, 1993: Modes of interannual tropical ocean–atmosphere interaction—A unified view. Part I: Numerical results. *J. Atmos. Sci.*, **50**, 3477–3503.
- Kirtman, B. P., and P. S. Schopf, 1998: Decadal variability in ENSO predictability and prediction. *J. Climate*, **11**, 2804–2822.
- McPhaden, M. J., and Coauthors, 1998: The tropical ocean global atmosphere observing system: A decade of progress. *J. Geophys. Res.*, **103**, 14 169–14 240.
- McCreary, J. P., and P. Lu, 1994: Interaction between the subtropical and equatorial ocean circulations—the subtropical cell. *J. Phys. Oceanogr.*, **24**, 466–497.
- Meehl, G. A., G. W. Branstator, and W. M. Washington, 1993: Tropical Pacific interannual variability and CO₂ climate change. *J. Climate*, **6**, 42–63.
- Moore, A. M., and R. Kleeman, 1997: The singular vectors of a coupled ocean–atmosphere model of ENSO. I. Thermodynamics, energetics and error growth. *Quart. J. Roy. Meteor. Soc.*, **123**, 953–981.
- , and —, 1999: Stochastic forcing of ENSO by the intraseasonal oscillation. *J. Climate*, **12**, 1199–1220.
- Munnich, M., M. A. Cane, and S. E. Zebiak, 1991: A study of self-excited oscillations of the tropical ocean–atmosphere system. Part II: Nonlinear cases. *J. Atmos. Sci.*, **48**, 1238–1248.
- Neelin, J. D., 1991: The slow sea surface temperature mode and the fast-wave limit—Analytic theory for tropical interannual oscillations and experiments in a hybrid coupled model. *J. Atmos. Sci.*, **48**, 584–606.
- , M. Latif, and F. F. Jin, 1994: Dynamics of coupled ocean–atmosphere models—The tropical problem. *Ann. Rev. Fluid Mech.*, **26**, 617–659.
- , D. S. Battisti, A. C. Hirst, F. F. Jin, Y. Wakato, T. Yamagata, and S. E. Zebiak, 1998: ENSO theory. *J. Geophys. Res.*, **103**, 14 261–14 290.
- Rajagopalan, B., U. Lall, and M. A. Cane, 1997: Anomalous ENSO occurrences: An alternate view. *J. Climate*, **10**, 2351–2357.
- Rasmusson, E. M., and T. H. Carpenter, 1982: The relationship between eastern equatorial Pacific sea surface temperatures and rainfall over India and Sri Lanka. *Mon. Wea. Rev.*, **110**, 354–384.
- , and J. M. Wallace, 1983: Meteorological aspects of the El Niño/Southern Oscillation. *Science*, **222**, 1195–1202.
- Rodbell, D. T., and Coauthors, 1999: An ~15,000-year record of El Niño–driven alluviation in southwestern Ecuador. *Science*, **283**, 516–519.
- Sandweiss, D. H., and Coauthors, 1996: Geoarchaeological evidence from Peru for a 5000 years BP onset of El Niño. *Science*, **273**, 1531–1533.
- Schopf, P. S., and M. J. Suarez, 1988: Vacillations in a coupled ocean–atmosphere model. *J. Atmos. Sci.*, **45**, 549–566.
- Schrag, D. P., G. Hampt, and D. W. Murray, 1996: Pore fluid constraints on the temperature and oxygen isotopic composition of the glacial ocean. *Science*, **272**, 1930–1932.
- Tett, S., 1995: Simulation of El Niño–Southern Oscillation-like variability in a global AOGCM and its response to CO₂ increase. *J. Climate*, **8**, 1473–1502.
- Thompson, C. J., and D. S. Battisti, 2000: A linear stochastic dynamical model of ENSO. Part I: Model development. *J. Climate*, **13**, 2818–2832.
- Timmermann, A., J. Oberhuber, A. Bacher, M. Esch, M. Latif, and E. Roeckner, 1999: Increased El Niño frequency in a climate model forced by future greenhouse warming. *Nature*, **398**, 694–697.
- Trenberth, K. E., and T. J. Hoar, 1997: El Niño and climate change. *Geophys. Res. Lett.*, **24**, 3057–3060.
- Wells, L. E., and J. S. Noller, 1997: Determining the early history of El Niño. *Science*, **276**, 966–966.
- Wunsch, C., 1999: The interpretation of short climate records, with comments on the North Atlantic and Southern Oscillations. *Bull. Amer. Meteor. Soc.*, **80**, 245–255.
- Zebiak, S. E., and M. A. Cane, 1987: A model El Niño–Southern Oscillation. *Mon. Wea. Rev.*, **115**, 2262–2278.
- Zhang, Y., J. M. Wallace, and D. S. Battisti, 1997: ENSO-like interdecadal variability: 1900–93. *J. Climate*, **10**, 1003–1020.